Structure and magnetic properties of RE_4CoCd and RE_4RhCd (RE = Tb, Dy, Ho)

2007 J. Phys.: Condens. Matter 19 076213

(http://iopscience.iop.org/0953-8984/19/7/076213)

IOP PUBLISHING JOURNAL OF PHYSICS: CONDENSED MATTER

J. Phys.: Condens. Matter **19** (2007) 076213 (13pp) doi:10.1088/0953-8984/19/7/076213

Structure and magnetic properties of RE_4CoCd and RE_4RhCd (RE = Tb, Dy, Ho)

Ahmet Doğan, Sudhindra Rayaprol and Rainer Pöttgen

Institut für Anorganische und Analytische Chemie, Westfälische Wilhelms-Universität Münster, Corrensstraße 30, 48149 Münster, Germany

E-mail: pottgen@uni-muenster.de

Received 17 October 2006, in final form 29 December 2006
Published 2 February 2007
Online at stacks.iop.org/JPhysCM/19/076213

Abstract

New rare earth metal rich cadmium compounds RE_4CoCd and RE_4RhCd (RE = Tb, Dy, Ho) were prepared by high-frequency melting of the elements in sealed tantalum tubes. The samples were studied by x-ray powder and single-crystal diffraction. All the compounds crystallize with Gd_4RhIn-type structure, with space group $F\bar{4}3m$. The structures are built up from rigid three-dimensional networks of condensed, cobalt (rhodium) centred trigonal RE_6 prisms. The voids left by these networks are filled by Cd_4 cluster units and the coordination number 14 polyhedra of the RE1 atoms. The terbium and dysprosium compounds in both series undergo antiferromagnetic ordering, whereas the holmium compounds exhibit ferromagnetic ordering. The magnetic ordering in these compounds is characterized by broad peaks around the transition temperatures. The results of detailed crystallographic investigations and preliminary magnetic and specific heat studies are presented and discussed in this work.

1. Introduction

The ternary RE–T–Cd systems (RE = rare earth metal, T = transition metal) have so far only scarcely been investigated. Complete phase analytical data have only been reported for the Ce–Cu–Cd system [1], revealing the ternary compounds $CeCu_{11-x}Cd_x$, $CeCu_{6-x}Cd_x$, $CeCu_{5-x}Cd_x$, $Ce_2Cu_5Cd_2$, $CeCuCd_2$, and CeCuCd. Further phase analytical investigations led to the intermetallic compounds $RECu_{5-x}Cd_x$ (RE = Ce, Gd, Tb, Yb) [2], $ErCuCd_2$ [3], the ordered Laves phases $CeNi_4Cd$ and $RECu_4Cd$ (RE = Ho, Er, Tm, Yb) [4], several equiatomic compounds RETCd (T = Pd, Ag, Au) (see [5–8], and references therein), $LaNiCd_2$ [9], $PrNiCd_2$, $LaPdCd_2$ [10], and a larger family of RE_2T_2Cd intermetallics (see [11–15], and references therein).

These cadmium intermetallics are highly interesting with respect to their magnetic and electrical properties. At least the RETCd and RE_2T_2Cd compounds crystallize with structures

that are typically observed for indides and stannides. Through substitution of indium or tin by cadmium within a given structure type, one can drastically change the valence electron concentration and thus influence the magnetic behaviour of the rare earth atoms. To give an example, GdAuCd [8] orders antiferromagnetically at $T_N = 66.5$ K, while GdAuIn [16] has the much lower ordering temperature of 12.5 K. Also Nd_2Pd_2Cd ($T_C = 23.7$ K) [15] has a significantly higher ordering temperature than Nd_2Pd_2In ($T_N = 7.5$ K) [17].

In view of these promising structure–property relationships, we have started a systematic study of the crystal chemistry and physical properties of $RE_xT_yCd_z$ intermetallics. Our recent phase analytical investigations revealed a series of new Gd_4RhIn-type compounds [18, 19]. The structure and magnetic properties of RE_4CoCd and RE_4RhCd (RE = Tb, Dy, Ho) are reported herein.

2. Experimental details

2.1. Synthesis

The starting materials for the preparation of the RE_4CoCd and RE_4RhCd (RE = Tb, Dy, Ho) samples were ingots of the rare earth elements (Johnson-Matthey or Kelpin), cobalt powder (Sigma-Aldrich, 100 mesh, >99.9%), rhodium powder (Degussa-Hüls, about 200 mesh), and a cadmium rod (Johnson-Matthey), all with a stated purity better than 99.9%. Pieces of the rare earth metals were first arc-melted into small buttons under purified argon. The elements were then weighed in 4:1:1 atomic ratio and sealed in small tantalum tubes under purified argon [20]. The tantalum ampoules were then placed in a water-cooled quartz sample chamber of a high-frequency furnace (Hüttinger Elektronik, Freiburg type TIG 1.5/300) under flowing argon [21] and first heated at 1670 K for about 1 min and then annealed at around 870 K for 2–4 h. The temperature was controlled through a Sensor Therm Methis MS09 pyrometer with an accuracy of ±30 K. The samples could easily be separated from the crucible material. No reaction with the containers was evident.

The bulk samples were investigated by energy-dispersive x-ray analysis (EDX) in a Leica 420 I scanning electron microscope using the rare earth trifluorides, cobalt, rhodium, and cadmium as standards. No impurity elements heavier than sodium (detection limit of the machine) could be detected. The analyses were in excellent agreement with the ideal 4:1:1 composition.

2.2. X-ray imaging plate data and structure refinements

The RE_4CoCd and RE_4RhCd samples were characterized by x-ray powder diffraction (Guinier technique) using Cu Kα_1 radiation and α-quartz ($a = 491.30$, $c = 540.46$ pm) as an internal standard. The cubic lattice parameters (tables 1 and 2) were obtained by least-squares refinements of the Guinier data. Proper indexing was ensured through comparison of the experimental patterns with calculated ones [22] taking the atomic positions of the structure refinements. The powder and single-crystal lattice parameters agreed well.

Small single crystals were isolated from the annealed samples by mechanical fragmentation. They were examined by Laue photographs on a Buerger camera (equipped with an imaging plate system Fujifilm BAS-1800) in order to check their suitability for intensity data collection. Intensity data of the Ho_4CoCd and Ho_4RhCd crystals were collected at room temperature on a four-circle diffractometer (CAD4) with graphite-monochromatized Mo Kα radiation (71.073 pm) and a scintillation counter with pulse height discrimination. The scans were performed in the $\omega/2\theta$ mode. Empirical absorption corrections were applied on the basis

Table 1. Crystal data and structure refinements for RE_4CoCd (RE = Tb, Dy, Ho), Gd_4RhIn type, space group $F\bar{4}3m$, Pearson symbol cF96, $Z = 16$.

Empirical formula	Tb_4CoCd	Dy_4CoCd	Ho_4CoCd
Molar mass (g mol^{-1})	807.01	821.33	831.05
Unit cell dimension, a (pm)	1346.5(2)	1341.0(3)	1334.9(2)
(Guinier data), V (nm^3)	2.4413	2.4115	2.3787
Calculated density (g cm^{-3})	8.78	9.05	9.28
Crystal size (μm^3)	$10 \times 30 \times 40$	$10 \times 10 \times 100$	$20 \times 20 \times 50$
Detector distance (mm)	60	60	—
Exposure time (min)	5	5	—
ω range, increment (deg)	0–180, 1.0	0–180, 1.0	—
Integr. Param. A, B, EMS	13.5, 3.5, 0.010	13.0, 3.0, 0.012	—
Transm. ratio (max/min)	1.88	1.46	5.03
Absorption coefficient (mm^{-1})	51.6	54.9	58.6
$F(000)$	5360	5424	5488
θ range (deg)	2–30	3–30	2–33
Range in hkl	$\pm18, \pm18, \pm18$	$\pm18, \pm18, \pm18$	$\pm20, \pm20, \pm20$
Total no. reflections	6439	5611	8614
Independent reflections	405 ($R_{int} = 0.0944$)	396 ($R_{int} = 0.1690$)	481 ($R_{int} = 0.1518$)
Reflections with $I > 2\sigma(I)$	326 ($R_{sigma} = 0.0621$)	265 ($R_{sigma} = 0.1138$)	421 ($R_{sigma} = 0.0380$)
Data/parameters	405/20	396/19	481/20
Goodness-of-fit on F^2	0.798	0.737	1.070
Final R indices [$I > 2\sigma(I)$]	$R1 = 0.0278$ $wR2 = 0.0449$	$R1 = 0.0333$ $wR2 = 0.0502$	$R1 = 0.0231$ $wR2 = 0.0348$
R indices (all data)	$R1 = 0.0389$ $wR2 = 0.0462$	$R1 = 0.0609$ $wR2 = 0.0542$	$R1 = 0.0319$ $wR2 = 0.0364$
Flack parameter	—	−0.08(11)	—
BASF	0.23(7)	—	0.38(3)
Extinction coefficient	0.000 106(7)	0.000 078(6)	0.000 031(3)
Largest diff. peak and hole (e Å^{-3})	2.68 and −2.05	2.53 and −2.96	1.49 and −1.83

of Ψ-scan data followed by spherical absorption corrections. Intensity data of Tb_4CoCd, Dy_4CoCd, Tb_4RhCd, and Dy_4RhCd were collected in oscillation mode on a Stoe IPDS-II image plate diffractometer using monochromatized Mo Kα radiation (71.073 pm). Numerical absorption corrections were applied to these data sets. All relevant crystallographic details are listed in tables 1 and 2.

The powder patterns already revealed isotypy of the cadmium compounds with the series of RE_4CoMg intermetallics [23]. All data sets were compatible with space group $F\bar{4}3m$. The atomic parameters of La_4CoMg [23] were taken as starting values and the structures were refined using SHELXL-97 (full-matrix least-squares on F_o^2) [24] with anisotropic atomic displacement parameters for all sites. As a check for the correct compositions, the occupancy parameters were refined in separate series of least-squares cycles. All sites were fully occupied within two standard uncertainties, and in the final cycles the ideal occupancies were assumed again. Refinement of the correct absolute structures was ensured through refinement of the Flack parameter [25, 26]. Most crystals were twinned by inversion. Final difference Fourier

Table 2. Crystal data and structure refinements for RE_4RhCd (RE = Tb, Dy, Ho), Gd_4RhIn type, space group $F\bar{4}3m$, Pearson symbol cF96, $Z = 16$.

Empirical formula	Tb_4RhCd	Dy_4RhCd	Ho_4RhCd
Molar mass (g mol^{-1})	850.99	865.31	875.03
Unit cell dimensions, a (pm)	1357.3(1)	1352.9(1)	1348.3(1)
(Guinier data), V (nm^3)	2.5005	2.4763	2.4511
Calculated density (g cm^{-3})	9.04	9.28	9.49
Crystal size (μm^3)	$10 \times 40 \times 100$	$10 \times 40 \times 60$	$10 \times 10 \times 40$
Detector distance (mm)	60	60	—
Exposure time (min)	5	5	—
ω range; increment (deg)	0–180, 1.0	0–180, 1.0	—
Integr. Param. A, B, EMS	13.5, 3.5, 0.012	13.5, 3.5, 0.012	—
Transm. ratio (max/min)	3.67	1.79	2.30
Absorption coefficient (mm^{-1})	50.4	53.5	56.9
$F(000)$	5648	5712	5776
θ range (deg)	3–30	2–35	2–30
Range in hkl	$\pm19, \pm19, \pm19$	$\pm21, \pm21, \pm21$	$\pm18, \pm18, \pm18$
Total no. reflections	5108	9460	7093
Independent reflections	412 ($R_{int} = 0.0831$)	593 ($R_{int} = 0.0620$)	405 ($R_{int} = 0.1196$)
Reflections with $I > 2\sigma(I)$	369 ($R_{sigma} = 0.0460$)	519 ($R_{sigma} = 0.0352$)	370 ($R_{sigma} = 0.0329$)
Data/parameters	412/20	593/20	405/20
Goodness-of-fit on F^2	1.088	0.991	1.150
Final R indices [$I > 2\sigma(I)$]	$R1 = 0.0350$ $wR2 = 0.0702$	$R1 = 0.0286$ $wR2 = 0.0570$	$R1 = 0.0203$ $wR2 = 0.0380$
R indices (all data)	$R1 = 0.0409$ $wR2 = 0.0715$	$R1 = 0.0349$ $wR2 = 0.0582$	$R1 = 0.0273$ $wR2 = 0.0404$
Flack parameter	—	—	—
BASF	0.40(5)	0.42(3)	0.13(3)
Extinction coefficient	0.000 09(1)	0.000 109(8)	0.000 110(7)
Largest diff. peak and hole (e Å^{-3})	3.83 and −2.85	2.67 and −3.16	1.81 and −1.47

syntheses revealed no significant residual peaks (tables 1 and 2). The refined positional parameters and interatomic distances (as an example for both holmium compounds) are listed in tables 3 and 4. Further details on the structure refinements are available[1].

2.3. Magnetic and specific heat measurements

Magnetism and specific heat measurements for the compounds of the series RE_4TCd (RE = Tb, Dy, Ho; T = Co, Rh) were carried out on a Quantum Design Physical Property Measurement System (QD-PPMS, USA) using *VSM* and *HC* options respectively.

[1] Details may be obtained from Fachinformationszentrum Karlsruhe, D-76344 Eggenstein-Leopoldshafen (Germany), by quoting the Registry Nos CSD-417043 (Tb_4CoCd), CSD-417044 (Dy_4CoCd), CSD-417045 (Ho_4CoCd), CSD-417046 (Tb_4RhCd), CSD-417047 (Dy_4RhCd), and CSD-417048 (Ho_4RhCd).

Table 3. Atomic coordinates and anisotropic displacement parameters (pm^2) for RE_4CoCd and RE_4RhCd (RE = Tb, Dy, Ho). The anisotropic displacement factor exponent takes the form $-2\pi^2[(ha^*)^2U_{11} + \cdots + 2hka^*b^*U_{12}]$. U_{eq} is defined as a third of the trace of the orthogonalized U_{ij} tensor.

Atom	Wyck. pos.	x	y	z	U_{11}	$U_{22} = U_{33}$	$U_{12} = U_{13}$	U_{23}	U_{eq}
Tb_4CoCd									
Tb1	24g	0.561 84(10)	1/4	1/4	72(7)	57(4)	0	−6(6)	62(3)
Tb2	24f	0.189 52(10)	0	0	53(6)	47(4)	0	−19(5)	49(3)
Tb3	16e	0.347 95(8)	x	x	57(3)	U_{11}	−6(4)	U_{12}	57(3)
Co	16e	0.141 2(2)	x	x	75(9)	U_{11}	−8(9)	U_{12}	75(9)
Cd	16e	0.579 77(10)	x	x	46(4)	U_{11}	−17(5)	U_{12}	46(4)
Dy_4CoCd									
Dy1	24g	0.562 09(17)	1/4	1/4	60(11)	58(6)	0	−20(10)	59(5)
Dy2	24f	0.189 26(18)	0	0	37(11)	49(6)	0	−1(9)	45(5)
Dy3	16e	0.347 95(13)	x	x	56(5)	U_{11}	−18(6)	U_{12}	56(5)
Co	16e	0.141 2(3)	x	x	61(14)	U_{11}	−16(15)	U_{12}	61(14)
Cd	16e	0.579 78(18)	x	x	47(7)	U_{11}	−27(8)	U_{12}	47(7)
Ho_4CoCd									
Ho1	24g	0.438 31(6)	3/4	3/4	109(4)	86(2)	0	−10(3)	94(2)
Ho2	24f	0.810 69(6)	0	0	67(3)	77(2)	0	−11(3)	74(2)
Ho3	16e	0.652 08(4)	x	x	84(2)	U_{11}	3(2)	U_{12}	84(2)
Co	16e	0.858 89(13)	x	x	120(5)	U_{11}	−27(6)	U_{12}	120(5)
Cd	16e	0.420 37(6)	x	x	82(3)	U_{11}	−11(3)	U_{12}	82(3)
Tb_4RhCd									
Tb1	24g	0.564 14(9)	1/4	1/4	72(6)	49(4)	0	−3(6)	56(3)
Tb2	24f	0.190 08(10)	0	0	51(6)	46(4)	0	−28(5)	48(3)
Tb3	16e	0.349 57(7)	x	x	49(4)	U_{11}	−1(3)	U_{12}	49(4)
Rh	16e	0.142 44(13)	x	x	63(5)	U_{11}	−12(6)	U_{12}	63(5)
Cd	16e	0.580 21(11)	x	x	56(4)	U_{11}	−7(5)	U_{12}	56(4)
Dy_4RhCd									
Dy1	24g	0.563 60(6)	1/4	1/4	76(3)	74(2)	0	−1(4)	75(2)
Dy2	24f	0.189 74(6)	0	0	68(3)	60(2)	0	−13(3)	62(2)
Dy3	16e	0.349 72(5)	x	x	65(2)	U_{11}	7(2)	U_{12}	65(2)
Rh	16e	0.142 48(8)	x	x	78(3)	U_{11}	−17(3)	U_{12}	78(3)
Cd	16e	0.580 14(7)	x	x	76(3)	U_{11}	−13(3)	U_{12}	76(3)
Ho_4RhCd									
Ho1	24g	0.436 42(5)	3/4	3/4	109(4)	108(2)	0	−4(4)	108(2)
Ho2	24f	0.810 45(6)	0	0	100(3)	93(2)	0	−10(3)	95(2)
Ho3	16e	0.650 09(4)	x	x	102(2)	U_{11}	13(2)	U_{12}	102(2)
Rh	16e	0.857 44(8)	x	x	113(3)	U_{11}	−13(4)	U_{12}	113(3)
Cd	16e	0.419 73(7)	x	x	117(3)	U_{11}	−7(3)	U_{12}	117(3)

3. Results and discussions

3.1. Crystal chemistry

Rare earth compounds RE_4CoCd and RE_4RhCd (RE = Tb, Dy, Ho) crystallize with the cubic Gd_4RhIn-type structure [18, 19]. This peculiar structure type has also been observed for the series of RE_4CoMg (RE = Y, La, Pr, Nd, Sm, Gd–Tm) compounds [23]. As an example, a view of the Ho_4RhCd structure is presented in figure 1. The structure contains two striking structural motifs. The rhodium atoms are coordinated in the form of slightly distorted trigonal prisms by the Ho2 and Ho3 atoms and these trigonal prisms are condensed via common corners to a three-dimensional network. The short Rh–Ho distances (279 and 280 pm) are indicative

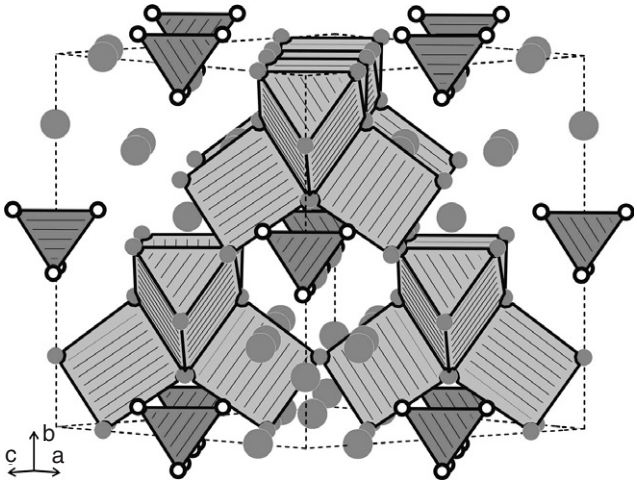

Figure 1. The crystal structure of Ho_4RhCd. Holmium, rhodium, and cadmium atoms are drawn as medium grey, filled (hidden in the trigonal prisms), and open circles, respectively. The three-dimensional network of corner-sharing $RhHo_6$ trigonal prisms and the Cd_4 tetrahedra is emphasized.

Table 4. Interatomic distances (pm), calculated with the powder lattice parameters of Ho_4CoCd and Ho_4RhCd. Standard deviations are given in parentheses. All distances within the first coordination spheres are listed.

Ho_4CoCd				Ho_4RhCd			
Ho1:	2	Cd	322.5(1)	Ho1:	2	Cd	324.2(1)
	2	Co	339.9(1)		2	Rh	345.3(1)
	2	Ho3	340.0(1)		2	Ho3	345.4(1)
	4	Ho2	353.2(1)		4	Ho2	355.5(1)
	4	Ho1	355.5(1)		4	Ho1	357.2(2)
Ho2:	2	Co	274.1(2)	Ho2:	2	Rh	279.1(1)
	2	Cd	343.1(1)		2	Cd	346.0(1)
	4	Ho1	353.2(1)		4	Ho1	357.2(1)
	2	Ho3	356.7(1)		2	Ho3	358.7(1)
	4	Ho2	357.4(1)		4	Ho2	361.4(1)
Ho3:	3	Co	276.9(2)	Ho3:	3	Rh	279.9(1)
	3	Cd	338.2(1)		3	Cd	337.9(1)
	3	Ho1	340.0(1)		3	Ho1	345.4(1)
	3	Ho2	356.7(1)		3	Ho2	358.7(1)
	3	Ho3	369.7(2)		3	Ho3	381.0(2)
Co:	3	Ho2	274.1(2)	Rh:	3	Ho2	279.1(1)
	3	Ho3	276.8(2)		3	Ho3	279.9(1)
	3	Ho1	339.9(1)		3	Ho1	345.3(1)
Cd:	3	Cd	300.7(2)	Cd:	3	Cd	306.1(3)
	3	Ho1	322.5(1)		3	Ho1	324.4(1)
	3	Ho3	338.2(1)		3	Ho3	337.9(1)
	3	Ho2	343.1(1)		3	Ho2	346.0(1)

for strong covalent bonding within these units, as was also evident from electronic structure calculations for isotypic La_4CoMg [23].

The voids left by the network of trigonal prisms are filled by cadmium tetrahedra that also show an *fcc* packing. The Cd–Cd distance of 306 pm is similar to the Cd–Cd distances in

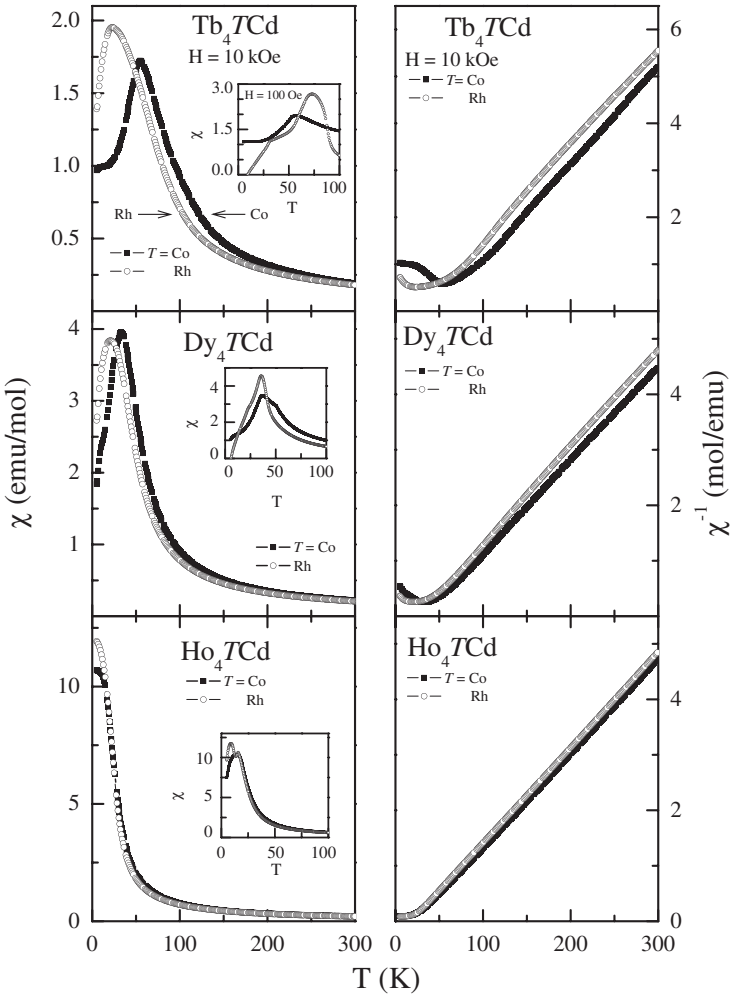

Figure 2. The dc susceptibility ($\chi = M/H$) measured for the RE_4TCd (RE = Tb, Dy and Ho; T = Co, Rh) series in $H = 10$ kOe field, plotted as χ and χ^{-1} versus T. The inset shows the low-field ($H = 100$ Oe) susceptibility measurement.

hcp cadmium (6 × 298 and 6 × 329 pm) [27], and we can assume a significant degree of Cd–Cd bonding within the tetrahedra. This is a very rare structural motif in solid-state materials. Further, voids are filled by the coordination number 14 polyhedra of the Ho1 atoms that are not part of the trigonal prismatic network. For further details on the crystal chemistry of these materials we refer to our recent work on the isotypic series of magnesium compounds [23].

Finally we need to return to the site occupancy parameters. There is a severe difference between the RE_4CoMg [23] and the RE_4CoCd/RE_4RhCd series. The RE1 positions that do not contribute to the trigonal prismatic network show significant RE1/Mg mixing in the RE_4CoMg series, while all sites are fully occupied within two standard uncertainties in the RE_4CoCd and RE_4RhCd series. This is an important point with respect to the magnetic properties, since the RE1/Mg mixing has a pronounced influence on the electron count, and thus the magnetic coupling between the three crystallographically independent RE sites. Detailed structural and

Table 5. Values of magnetic ordering temperatures (determined from $d\chi/dT$), effective Bohr magneton and paramagnetic Curie temperatures for RE_4TCd compounds determined from susceptibility measurements.

Compound	Ordering temperature (K)	μ_{eff} (μ_B/RE atom)	θ_p (K)
Tb_4CoCd	54(1)	9.74(2)	52.5(5)
Dy_4CoCd	34(1)	10.87(2)	33.5(5)
Ho_4CoCd	24(1)	10.79(2)	24.1(5)
Tb_4RhCd	22(1)	10.03(2)	19.7(5)
Dy_4RhCd	21(1)	10.69(2)	24.9(5)
Ho_4RhCd	22(1)	10.75(2)	18.8(5)

magnetic investigations of representative solid solutions $RE_{4-x}CoMg_{1+x}$ and $RE_{4-x}RhMg_{1+x}$ are currently in progress.

3.2. The dc susceptibility ($\chi = M/H$)

In figure 2, we show the magnetic susceptibility, $\chi(=M/H)$ measured in a field of 10 kOe for RE_4TCd (RE = Tb, Dy and Ho; T = Co, Rh). The inverse susceptibility is also plotted in the same figure to highlight the Curie–Weiss behaviour at high temperatures (in 100–300 K range). The $\chi(T)$ plots clearly show the antiferromagnetic ordering, T_N at 54(1) and 34(1) K for Tb_4CoCd and Dy_4CoCd respectively. Ho_4CoCd undergoes ferromagnetic ordering, T_C at 24(1) K (T_C determined from $d\chi/dT$). From the plot of χ^{-1} versus T, the values of the paramagnetic Curie temperature (θ_p) and the Bohr magneton number (μ_{eff}) were calculated, and they are shown in table 5. For all three compounds of the RE_4CoCd series, the values of μ_{eff} are close to the expected free ion values.

A close look at the $\chi(T)$ behaviour below 100 K shows that for the Tb and the Dy compound there is a possibility of another magnetic transition around 5 K, also seen in low-field measurements (inset of figure 2). χ for the Ho compound appears to be saturating below 5 K. The antiferromagnetic ordering in the Tb and the Dy compounds is clearly seen as a peak around their respective transition temperatures; however, in the case of Ho_4CoCd, T_C is not clearly evident from $\chi(T)$ alone as the onset takes place at a temperature as high as 60 K. It should also be noted here that χ^{-1} flattens below 25 K for Ho_4CoCd.

Now we focus on the physical properties of the RE_4RhCd series. The crystallographic studies clearly show that, on moving from Co to Rh, there is definitive change in the volume (owing to the larger ionic radii of Rh compared to Co), also affecting the magnetism of these compounds. In figure 2 we also show the susceptibility behaviour for the compounds of the RE_4RhCd series (RE = Tb, Dy and Ho) measured in $H = 10$ kOe. The differences in the magnetism in the RE_4CoCd and RE_4RhCd series is clearly evident from their $\chi(T)$ behaviour. The peaks around the ordering temperatures in the RE_4RhCd series (for RE = Tb and Dy) are broader as compared to the compounds of the Co series (figure 2). In the RE_4RhCd series also, the Tb and Dy compounds undergo antiferromagnetic ordering at 22(1) and 21(1) K respectively, and Ho_4RhCd orders ferromagnetically at 22(1) K. The values of θ_p and μ_{eff}, obtained from the linear region (100–300 K) in the χ^{-1} versus T plots, are listed in table 5. The values of μ_{eff} for the RE_4RhCd compounds are also close to the expected values for the free RE^{3+} ions.

3.3. Magnetization (M versus H)

We have also studied the magnetization behaviour of these interesting compounds up to fields of 80 kOe at 5 K, i.e., well below their respective magnetic ordering temperatures. The

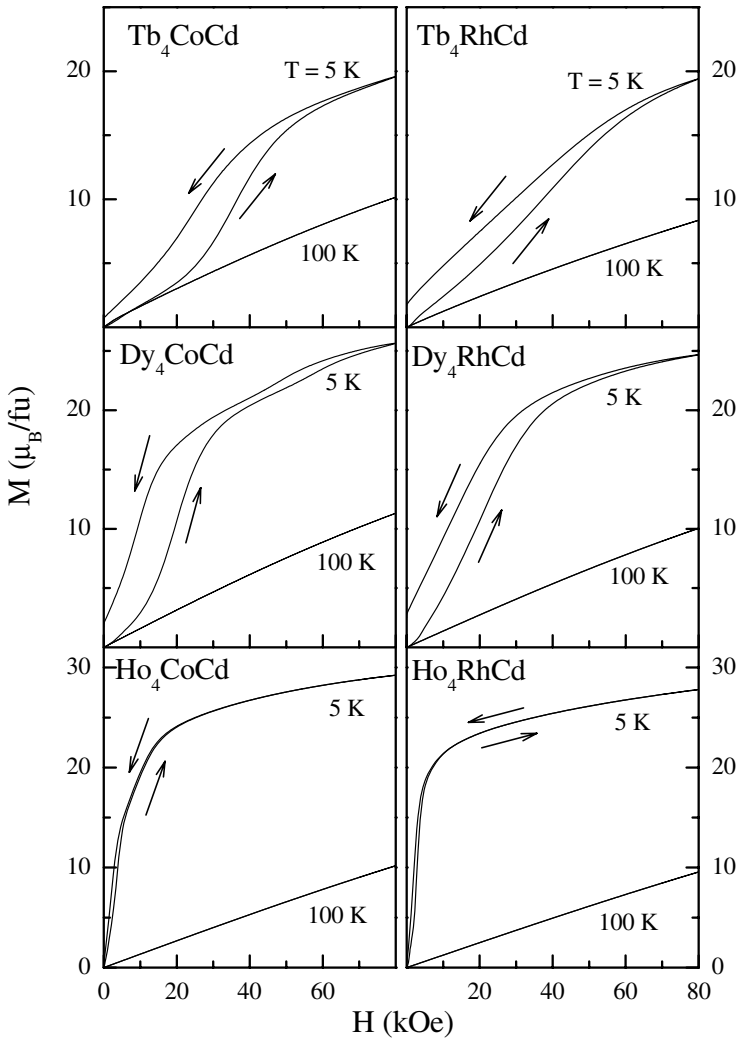

Figure 3. Magnetization as a function of field (M versus H) measured at $T = 5$ and 100 K for compounds of the RE_4CoCd and RE_4RhCd series. The arrows indicate the direction of field sweeping.

magnetization measurements, up to 80 kOe, as well as low-field hysteresis loops measured in fields of ±10 kOe, are also shown in figures 3 and 4 respectively. In figure 3 we show the magnetization (M–H) behaviour for RE_4CoCd at 5 and 100 K. $M(H)$ for Tb_4CoCd increases linearly with H for initial application of field (for $H < 20$ kOe), increases dramatically as H approaches 20 kOe, exhibiting a metamagnetic transition as H crosses this critical field of about 20 kOe, and increases with further increase in H. The compound exhibits large hysteresis, when the field is ramped down from 80 to 0 kOe. This feature can also be clearly seen in the hysteresis loop measured at 5 K in fields between ±10 kOe (figure 4).

For Dy_4CoCd, a field-induced transition takes place even with a small field, as can be clearly seen from the $M(H)$ at 5 K (figure 3). The continuous change in M with H continues up to 25 kOe, and then M varies linearly with increasing H. $M(H)$ of Dy_4CoCd at 5 K also

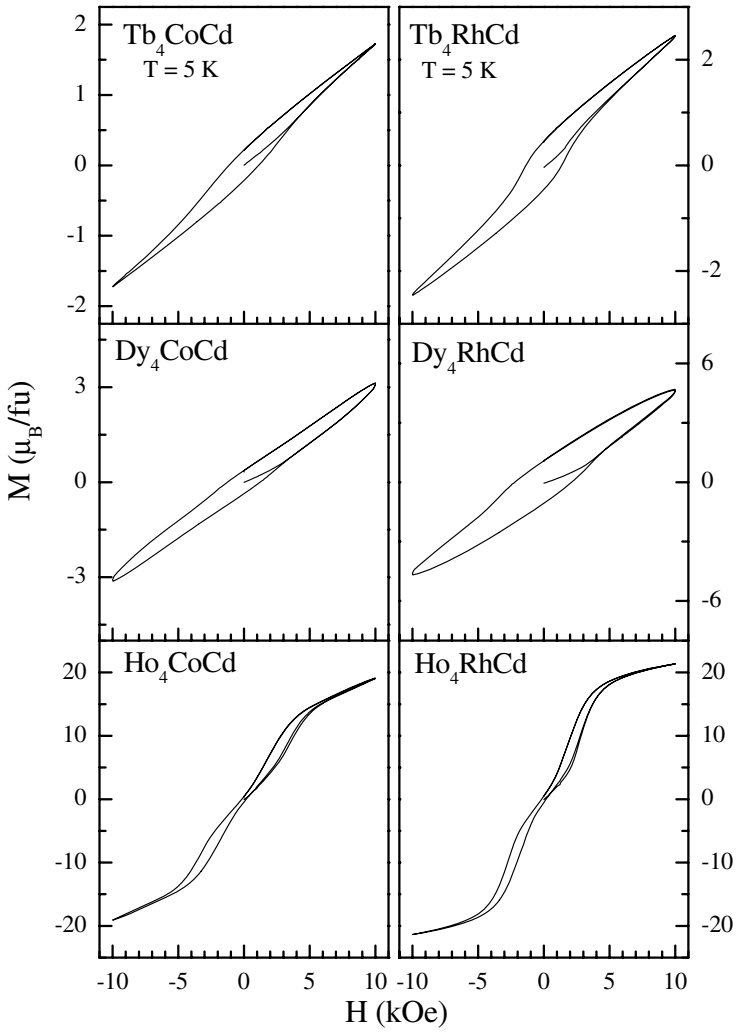

Figure 4. Hysteresis loops measured at 5 K for compounds of the RE_4CoCd and RE_4RhCd series.

exhibits hysteresis as the field is reversed to 0 from 80 kOe. Also, the low-field hysteresis loop (figure 4) clearly shows such a behaviour for Dy_4CoCd.

$M(H)$ for Ho_4CoCd at 5 K increases sharply with a small change in H, confirming the spontaneous moment in this system, consistent with the observation of ferromagnetic ordering. However, above 20 kOe, M varies rather sluggishly with increasing H. The hysteresis loop measured at 5 K for Ho_4CoCd exhibits a metamagnetic transition between 0 and 5 kOe in both directions of the field sweeping. The hysteresis loop also exhibits broadening of the loop between 0 and 5 kOe. From its magnetization behaviour, Ho_4CoCd can be classified as a soft ferromagnet (coercive field, $H_C = 186$ Oe). $M(H)$ for Tb_4RhCd is different from that of the isostructural compound Tb_4CoCd at 5 K. In Tb_4RhCd, also, M experiences a metamagnetic transition at smaller fields. M varies sluggishly with H up to 60 kOe. M deviates from this behaviour between 60 and 80 kOe and appears to be curved. Here also large hysteresis is observed when the field is ramped down from 80 to 0 kOe, which is clearly seen in the hysteresis loop (figure 4) measured at the same temperature.

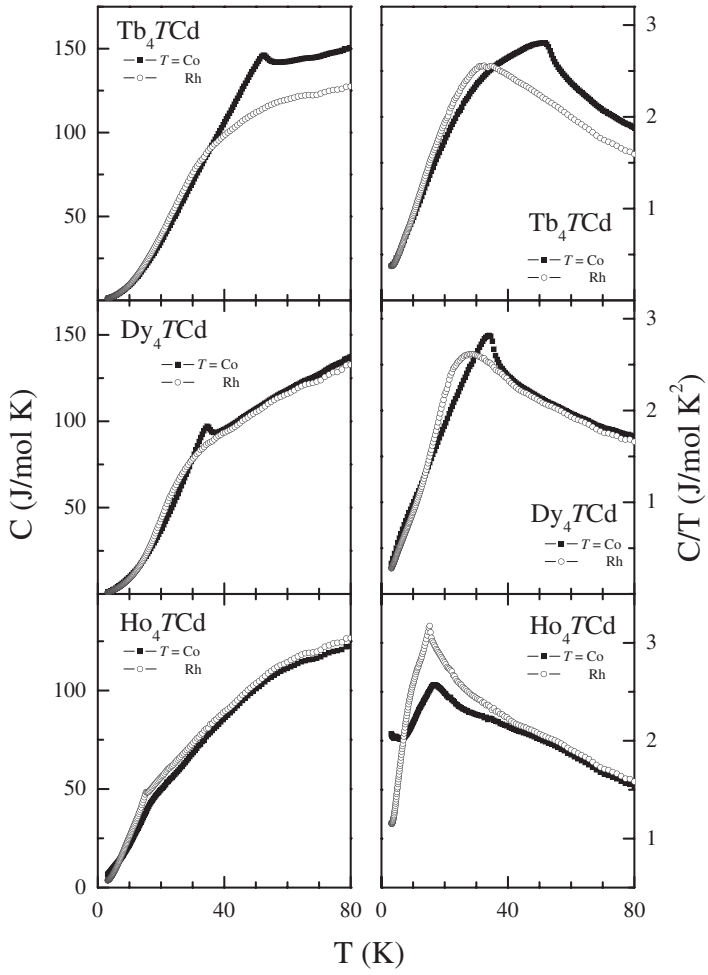

Figure 5. Specific heat data plotted in different forms for the RE_4TCd (RE = Tb, Dy and Ho; T = Co, Rh) series.

The behaviour of $M(H)$ at 5 K for Dy_4RhCd is also slightly different from that of its counterpart in the Co series, Dy_4CoCd. M increases almost linearly with H up to 40 kOe, and deviates as H approaches 80 kOe. The field-induced transition seen in Dy_4CoCd is absent here; however, like the former compound, Dy_4RhCd also exhibits large hysteresis effects (also seen in figure 4).

The $M(H)$ for Ho_4RhCd resembles, for the most part, that of Ho_4CoCd, except for the features between 5 and 15 kOe. A small change in H results in a sharp rise in M, presumably due to a spontaneous magnetization in this ferromagnetically ordered compound. Above 10 kOe, M increases linearly with increasing H with a tendency to saturate at higher fields. The hysteresis loop measured at the same temperature clearly shows that Ho_4RhCd also undergoes a field-induced transition at low fields (between 0 and 5 kOe). Owing to these characteristics of the magnetization curve, Ho_4RhCd can also be classified as a soft ferromagnet ($H_C = 160$ Oe).

The saturation magnetization for the Tb compounds at 5 K in both series is about 55% of the expected value (given by $g \times J = 9.0\ \mu_B\ mol^{-1}$ for Tb, $J = 6$) at 80 kOe. Similarly, for the Dy and Ho compounds (in both series) M reaches about 60 and 70% of the expected

saturation magnetization value at 80 kOe at 5 K. The discrepancy in the observed and expected values can be attributed to the crystal field effects and/or the polycrystalline character of the samples. Also it is possible that a field strength of 80 kOe is insufficient for the saturation of the moments.

At 100 K for all compounds of the RE_4TCd (T = Co, Rh) series, M varies linearly with H, indicating the paramagnetic state of the samples, confirming the observations made in the susceptibility measurements.

3.4. Specific heat studies

In order to get a precise idea about the magnetic ordering temperatures, we have performed specific heat measurements in the 3–100 K range. The plots of C and C/T versus T are shown in figure 5 for the RE_4CoCd series. For both antiferromagnetic compounds, i.e., Tb_4CoCd and Dy_4CoCd, there is a prominent λ-type peak at 52(1) and 34(1) K respectively, corresponding to the ordering temperatures observed from susceptibility measurements. For Ho_4CoCd, there is a small change in the plot of $C(T)$ around 17(1) K. This anomaly can be seen more clearly from the plot of C/T versus T. However, the λ-anomaly is missing in this compound. There is an upturn in C/T below 5 K, possibly indicating the presence of another magnetic transition.

In figure 5 we have also shown the specific heat data (as C and C/T versus T) for the RE_4RhCd series. In contrast to the Co series, neither $C(T)$ nor C/T versus T exhibits any clear λ-anomaly around the ordering temperatures (determined from the magnetic measurements) in the compounds of the Rh series. There is a broad peak-like feature in C/T versus T for the Tb and Dy compounds. However, in the case of Ho_4RhCd, a sharp drop in $C(T)$ and a peak in C/T versus T characterizes the ordering temperature. It should be noted here that, like Ho_4CoCd, Ho_4RhCd also exhibits an upturn in C/T versus T below 5 K indicating another magnetic transitions around or below this temperature.

4. Conclusions

The series of isostructural RE_4CoCd and RE_4RhCd compounds with RE = Tb, Dy, and Ho was synthesized and structurally characterized. The magnetic and specific heat measurements on a series of RE_4TCd compounds (RE = Tb Dy and Ho; T = Co, Rh) exhibits interesting magnetic properties. Magnetic ordering was detected for all the compounds, antiferromagnetic ordering for the terbium and the dysprosium compounds, and ferromagnetism in the holmium compounds. The magnetic transitions in both series are characterized by broad peaks in the susceptibility measurements. The broad peaks are intrinsic to these compounds, as can also be seen in the low-field (H = 100 Oe) measurements. The ordering temperatures decrease when Co is replaced by Rh at the transition metal site, indicating that both volume (structural) and electron count (3d versus 4d) may be responsible for governing the magnetic properties in these isostructural compounds. The low-temperature magnetization curves are very interesting. Another point for further investigations is the discrepancies seen in the ordering temperatures in the susceptibility and specific heat measurements. Though it is difficult to precisely determine the ordering temperatures in susceptibility measurements owing to broad peaks, the values of T_N determined from $\mathrm{d}\chi/\mathrm{d}T$ is close to the ordering temperatures observed from $C(T)$ curves in the case of the Tb and Dy compounds of the RE_4CoCd series. Similar observations are made for the RE_4RhCd series also. However, in the case of both Ho compounds, there is a difference of about 6 K in T_C determined from susceptibility and specific heat measurements.

Finally, we believe the present work on the precise structural determination and preliminary investigations on the magnetic behaviour of RE_4TCd (RE = Tb, Dy, Ho; T = Co,

Rh) type intermetallics with be followed by further work, both experimental and theoretical, in understanding the physical properties of these highly interesting compounds, particularly at temperatures below 100 K. We believe that temperature-dependent neutron diffraction measurements will be rewarding in understanding in detail the magnetic unit cell, and thus the origin of magnetic interaction in these compounds which could enable us to correlate the structural and physical properties.

Acknowledgments

We thank Dipl.-Ing. U Ch Rodewald for help with the intensity data collection. This work was supported by the Deutsche Forschungsgemeinschaft. SR is indebted to the Alexander von Humboldt Foundation for a postdoctoral stipend.

References

[1] Horechyy A I, Pavlyuk V V and Bodak O I 1999 *Pol. J. Chem.* **73** 1681
[2] Pavlyuk V V, Horechyj A I, Kevorkov D G, Dmytriv G S, Bodak O I, Koziol J J, Ciesielski W and Kapuśniak J 2000 *J. Alloys Compounds* **296** 276
[3] Zelinska O Ya, Solokha P G and Pavlyuk V V 2004 *J. Alloys Compounds* **367** 176
[4] Doğan A and Pöttgen R 2005 *Z. Naturf.* b **60** 495
[5] Mishra R, Pöttgen R, Hoffmann R-D, Kaczorowski D, Piotrowski H, Mayer P, Rosenhahn C and Mosel B D 2001 *Z. Anorg. Allg. Chem.* **627** 1283
[6] Fickenscher Th, Kotzyba G, Hoffmann R-D and Pöttgen R 2001 *Z. Naturf.* b **56** 598
[7] Fickenscher Th, Hoffmann R-D, Mishra R and Pöttgen R 2002 *Z. Naturf.* b **57** 275
[8] Łątka K, Kmieć R, Pacyna A W, Fickenscher Th, Hoffmann R-D and Pöttgen R 2004 *J. Magn. Magn. Mater.* **280** 90
[9] Doğan A, Johrendt D and Pöttgen R 2005 *Z. Anorg. Allg. Chem.* **631** 451
[10] Doğan A, Rodewald U Ch and Pöttgen R 2006 *Z. Naturf.* b **61** at press
[11] Lukachuk M and Pöttgen R 2003 *Z. Kristallogr.* **218** 767
[12] Fickenscher Th, Rodewald U Ch, Niepmann D, Mishra R, Eschen M and Pöttgen R 2005 *Z. Naturf.* b **60** 271
[13] Rayaprol S and Pöttgen R 2005 *Phys. Rev.* B **72** 214435
[14] Rayaprol S and Pöttgen R 2006 *Phys. Rev.* B **73** 214403
[15] Rayaprol S, Doğan A and Pöttgen R 2006 *J. Phys.: Condens. Matter* **18** 5473
[16] Pöttgen R, Kotzyba G, Görlich E A, Łątka K and Dronskowski R 1998 *J. Solid State Chem.* **141** 352
[17] Giovannini M, Michor H, Bauer E, Hilscher G, Rogl P and Ferro R 1998 *J. Alloys Compounds* **280** 26
[18] Zaremba R, Rodewald U Ch and Pöttgen R 2006 *Z. Kristallogr. (Suppl.)* **14** 161
[19] Zaremba R, Rodewald U Ch and Pöttgen R 2006 *Z. Anorg. Allg. Chem.* **632** 2106
[20] Pöttgen R, Gulden Th and Simon A 1999 *GIT Labor-Fachz.* **43** 133
[21] Kußmann D, Hoffmann R-D and Pöttgen R 1998 *Z. Anorg. Allg. Chem.* **624** 1727
[22] Yvon K, Jeitschko W and Parthé E 1977 *J. Appl. Crystallogr.* **10** 73
[23] Tuncel S, Hoffmann R-D, Chevalier B, Matar S F and Pöttgen R 2007 *Z. Anorg. Allg. Chem.* **633** 151
[24] Sheldrick G M 1997 *SHELXL-97, Program for Crystal Structure Refinement* University of Göttingen
[25] Flack H D and Bernadinelli G 1999 *Acta Crystallogr.* A **55** 908
[26] Flack H D and Bernadinelli G 2000 *J. Appl. Crystallogr.* **33** 1143
[27] Donohue J 1974 *The Structures of the Elements* (New York: Wiley)